www.revistageintec.net
ISSN: 2237-0722
revista GEINTEC
Gestão, Inovação e Tecnologias

Modeling of Buck ZVS Multiresonant DC-DC Converter Using Bond Graphs

Shaik Hussain Vali[1*]; R. Kiranmayi[2]
[1*]Research Scholar, EEE Department, JNTU Anantapur, Anantapuramu, Andhra Pradesh, India.
[1*]hussainvali4@gmail.com
[2]Professor, EEE Department, JNTUA CE, Anantapuramu, Andhra Pradesh, India.

Abstract
Pulse width modulated (PWM) converters are suffering from poor efficiency due to high switching losses. quasiresonant converters with the help of resonance phenomenon can come to the rescue of PWM converters. There are certain problems even with the quasiresonant converters. Problems with quasiresonant converters such as parasitic oscillations and high voltage stress can be resolved with the help of multiresonant converters. Appropriate modeling technique is needed to accurately represent the physical system. The multiresonant converters along with electrical systems are involved in magnetic and thermal systems. For this kind of systems, the appropriate modeling is bond graph. In this piece of work, buck ZVS multiresonant converter is taken to model using bond graphs. The large signal bond graph model is created. In MATLAB/SIMULINK for state variables the created bond graph model is simulated. The findings obtained are checked with PSIM simulated results and experimental results. The comparison of model and experimental results prove the model's accuracy.

Key-words: Bond Graph, Buck, Modeling, Multiresonant, Zero Voltage Switching.

1. Introduction

Contrary to linear regulators, the PWM converters are more effective, compact in size [1-3]. Yet they suffer from heavy switching losses and issues with electromagnetic interference. The high frequency necessity results in the creation of Quasiresonant converters (QRC), utilising zero voltage (ZVS) and zero current (ZCS) switching techniques, helping to solve the above-mentioned issues [4-6]. But these ZCS converters are effective up to about 2MHz operating frequency. In addition to this frequency ZCS converters are challenging to use due to capacitive losses and parasitic oscillations. ZVS QRCs can address these problems up to a 10 MHz switching frequency. But ZVS QRCs have problems with high voltage stress, narrow load changes and stability issues on the switches. Multiresonant converters can solve these problems by providing resonant stages over one cycle [7].

For effective device modeling, the system should be well-defined. In the case of electrical power converters, various modeling techniques are built on the basis of requirements [8-11]. They include switched state-space model, average state-space model, average circuit model, generalized average model, sampled data models [9] etc. Challenges in modeling are the development of models to minimize simulation time, the development of models for basic elements to fit simulation, simulation duration, consistency of the outcome, precision of the result. If the system is static or dynamic, this defines the modeling form. The PSPICE is primarily used for switched mode power converters with readymade blocks. There are numerous simulation approaches usable, such as the Global Simulation Method, the Method of Parity Simulation, and the Sequential Simulation Method.

The ZVS buck multiresonant DC-DC converter is a dynamic system of more than one domain. It includes thermal, mechanical and magnetic fields, aside from electrical. Modeling such multi-domain structures typically requires a dynamic process. It is carried out by transforming the non-electrical areas into their equal analogous electrical domains and converting the virtual effects to the initial domain result again. Bond Graph modeling [12-14] may be used to some degree for rescue purposes. The methodology of bond-graph modeling is more advantageous for multi-domain modeling. It functions on the power or energy vector common to any domain. No analogous systems are needed.

2. Bond Graph Modeling Approach

Bond graphs [12-14] depict structures in the form of pictures. The diagram includes several bonds and many intersections. Each bond has some direction. Each bond has two variables: effort and flow. The bond directions are determined by causality. The junctions are 0 and 1 junctions. The bond graph is based on the system's activity. If the graph is finished, the state equations are derived from the simple operating laws of the system. The bond graph modeling is relevant to the power electronic converter systems [15, 16]. Switched power junctions (SPJ)[17] concept is useful for switched-mode power converters (SMPCs), since they require more switches with multiple switching combinations. They are junctions with 0s and 1s. For this the bond graph and its causality would stay the same regardless of switching combinations. The large signal, small signal and steady state models are developed. Thereafter, state equations are derived. This methodology unifies SMPC's large signal, small-signal, and steady-state models [18]. The same technique may be used for continuous and discontinuous operating modes.

3. Modeling of the Converter

Fig.1 displays the circuit of the Buck ZVS multi-resonant DC-DC converter (MRC)[7]. In these two resonant capacitors, each of them connected via a switch and a diode. The diode and capacitor combination in series is connected to a resonant inductor. If the effort value differs with switch locations, a 0 junction is substituted with a 0s junction. Similarly there is 1s-junction.

Fig. 1 - Buck ZVS Multiresonant DC-DC Converter

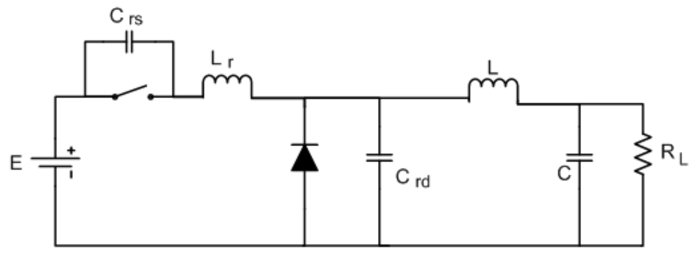

Fig. 2(a) - 2(d) display bond graph models [18] for various switch and diode combinations. Tabulate current and voltage variables with all these potential variations in Table 1 to Table 4. Fig. 2(e) displays the complete large signal bond graph. The state equations obtained from the bond graph are given from (1) to (5). Here, i_L, i_{Lr} ,v_C, v_{Crs} and v_{Crd} are filter inductor current, resonant inductor current, output voltage, resonant capacitor voltage across switch and resonant capacitor voltage across diode respectively and all are instantaneous values. They are taken as state variables. Whereas I_L, I_{Lr}, V_C, V_{Crs} and V_{Crd} are respectively filter inductor current, resonant inductor current, output voltage, resonant capacitor voltage across switch and resonant capacitor voltage across diode and all are steady state values.

Fig. 2(a) - Bond graph of Buck ZVS MRC when switch and diode are ON

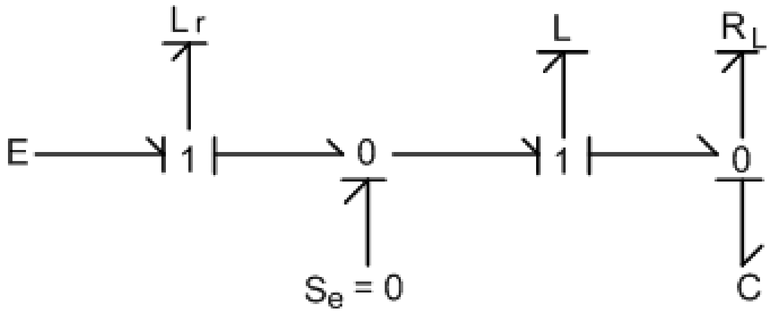

ISSN: 2237-0722
Vol. 11 No. 4 (2021)
Received: 19.05.2021 – Accepted: 11.06.2021

Fig. 2(b) - Bond graph of Buck ZVS MRC when switch is ON and diode is OFF

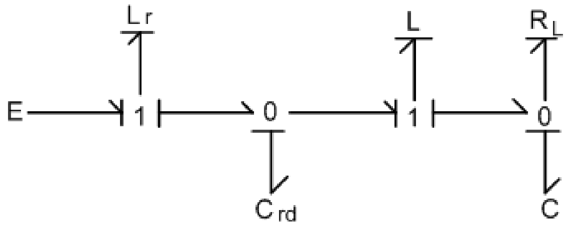

Fig. 2(c) - Bond graph of Buck ZVS MRC when switch and diode are OFF

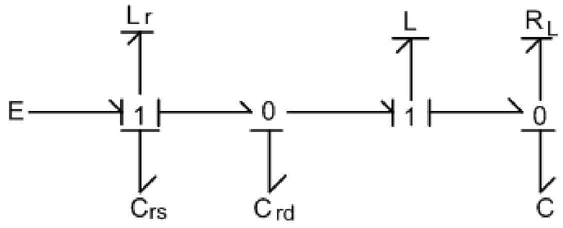

Fig. 2(d) - Bond graph of Buck ZVS MRC when switch is OFF and diode is ON

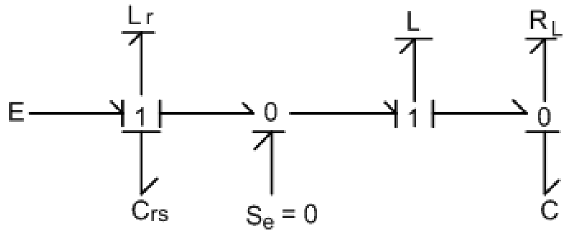

Table 1 - Variable values when both switch and diode are ON

Variable	V_{Lr}	V_L	I_{Crs}	I_{Crd}	I_C
Value	E	$- V_C$	0	0	$I_L - V_C / R_L$

Table 2 - Variable values when switch is ON and diode is OFF

Variable	V_{Lr}	V_L	I_{Crs}	I_{Crd}	I_C
Value	$E - V_{Crd}$	$V_{Crd} - V_C$	0	$I_{Lr} - I_L$	$I_L - V_C / R_L$

Table 3 - Variable values when both switch and diode are OFF

Variable	V_{Lr}	V_L	I_{Crs}	I_{Crd}	I_C
Value	$E - V_{Cs} - V_{Crd}$	$V_{Crd} - V_C$	I_{Lr}	$I_{Lr} - I_L$	$I_L - V_C / R_L$

Table 4 - Variable values when the switch is OFF and diode is ON

Variable	V_{Lr}	V_L	I_{Crs}	I_{Crd}	I_C
Value	$E - V_{Crs}$	$- V_C$	I_{Lr}	0	$I_L - V_C / R_L$

Fig. 2(e) - Large signal Bond graph of Buck ZVS MRC

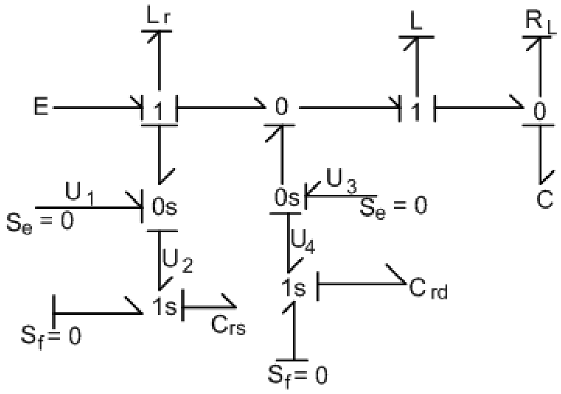

$$i_{Crs} = U_2 i_{Lr} \tag{1}$$

$$i_C = i_L - {v_C}/{R_L} \tag{2}$$

$$i_{Crd} = U_4 (i_{Lr} - i_L) \tag{3}$$

$$v_{Lr} = E - U_4 v_{Crd} - U_2 v_{Crs} \tag{4}$$

$$v_L = -v_C + U_4 v_{Crd} \tag{5}$$

4. Design of the Converter

Equations (6) to (8) are the expressions for desired load voltage (V_C), filter inductor (L), filter capacitance (C) and resonant frequency (f_o) in terms of supply input voltage (E), duty ratio (d), switching time period (T_s), switching frequency (f_s), Resistive load (R_L), percentage current ripple and percentage voltage ripple [3]. Equations (9) to (12) are the expressions for resonant inductor (L_r) and resonant capacitors across converter switch (C_{rs}) and converter diode (C_{rd}) respectively in terms of supply input voltage (E), duty ratio (d), resonant frequency (f_o) and Resistive load (R_L) [19]. The expressions are obtained by following the working principles of converter.

$$V_C = Ed \tag{6}$$

$$L = \frac{T_S R_L (1-d)}{\%currentripple} \tag{7}$$

$$C = \frac{{T_S}^2 (1-d)}{8L(\%vltageripple)} \tag{8}$$

$$f_0 = \frac{0.9092 E f_s}{E - V_C} \tag{9}$$

ISSN: 2237-0722
Vol. 11 No. 4 (2021)
Received: 19.05.2021 – Accepted: 11.06.2021

$$L_r = \frac{0.159ER_L}{V_C f_0} \tag{10}$$

$$C_{rs} = \frac{0.159V_C}{R_L E f_0} \tag{11}$$

$$C_{rd} = 4C_{rs} \tag{12}$$

The design parameters based on above equations, are shown in Table 5

Table 5 - Converter design Parameters

Input supply Voltage (E)	*20 V*
Load Voltage (V_c)	*14 V*
Resistive Load (R_L)	*100Ω*
Converter Switching Frequency (f_s)	*20000 Hz*
Resonant Frequency (f_o)	*60613 Hz*
Filter Inductance (L)	*0.15 H*
Filter Capacitance (C)	*300 μF*
Resonant Inductor (L_r)	*375 μH*
Resonant Capacitance across converter switch (C_{rs})	*18.38 nF*
Resonant Capacitance across converter diode (C_{rd})	*76 nF*

5. Simulated Results and Analysis

To build the SIMULINK diagram, a toolbox [20] is used to transform bond diagrams into MATLAB/SIMULINK software to model waveforms of current in filter inductor (i_L), current in resonant inductor (i_{Lr}), voltage across filter capacitor (v_c), voltage across switch resonant capacitor (v_{crs}) and voltage across diode resonant capacitor (v_{crd}) that are shown in Fig. 3(a) to 3(e).

Fig. 3(a) - Filter Inductor Current (I_L) of Buck ZVS MRC

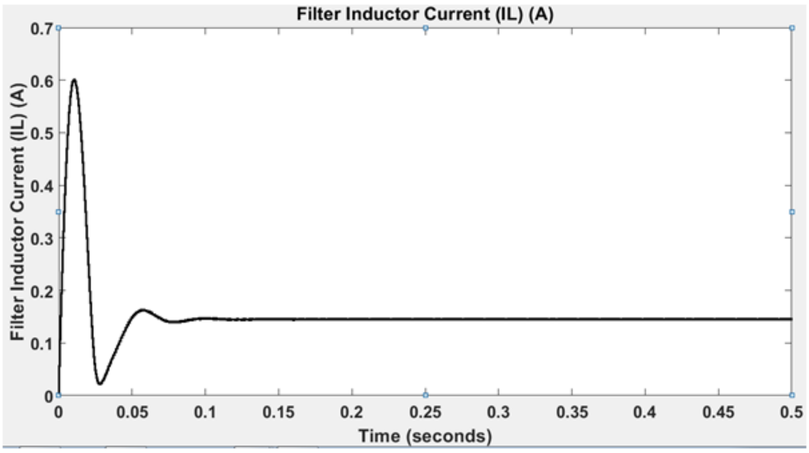

ISSN: 2237-0722
Vol. 11 No. 4 (2021)
Received: 19.05.2021 – Accepted: 11.06.2021

Fig. 3(b) - Resonant Inductor Current (I_{Lr}) of Buck ZVS MRC

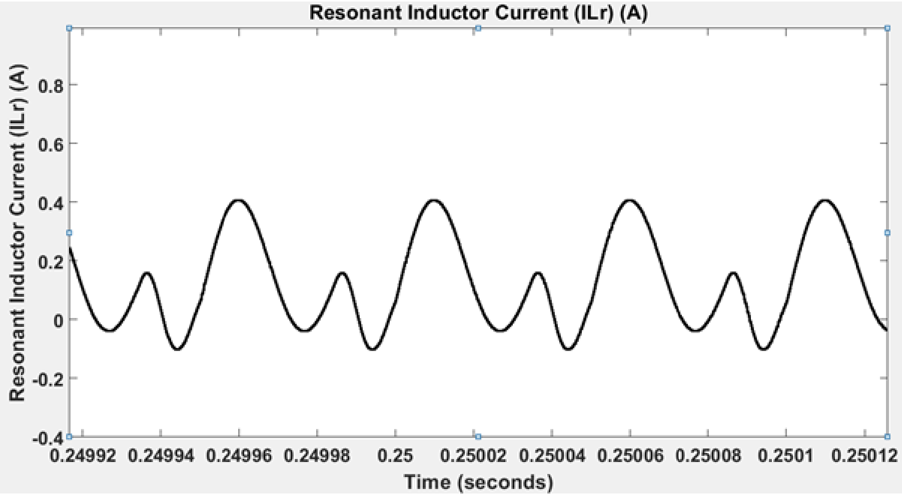

Fig. 3(c) - Filter Capacitor voltage (V_c) of Buck ZVS MRC

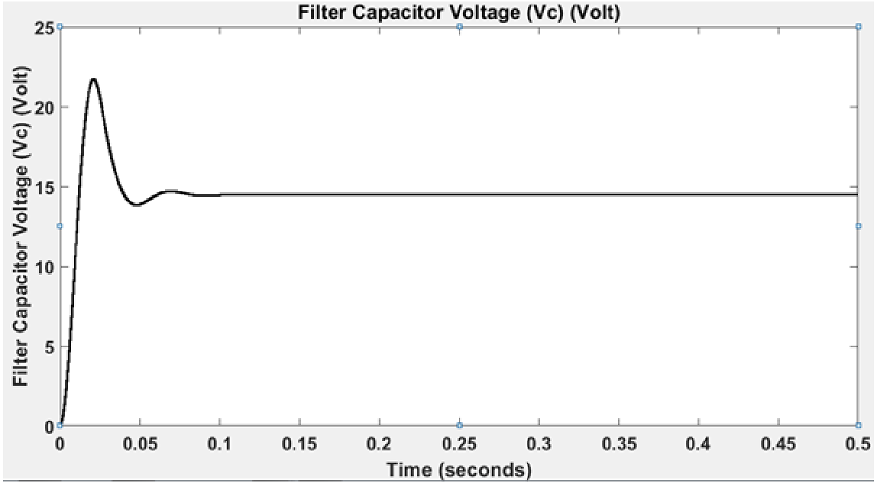

Fig. 3(d) - Resonant Voltage across switch (V_{crs}) of Buck ZVS MRC

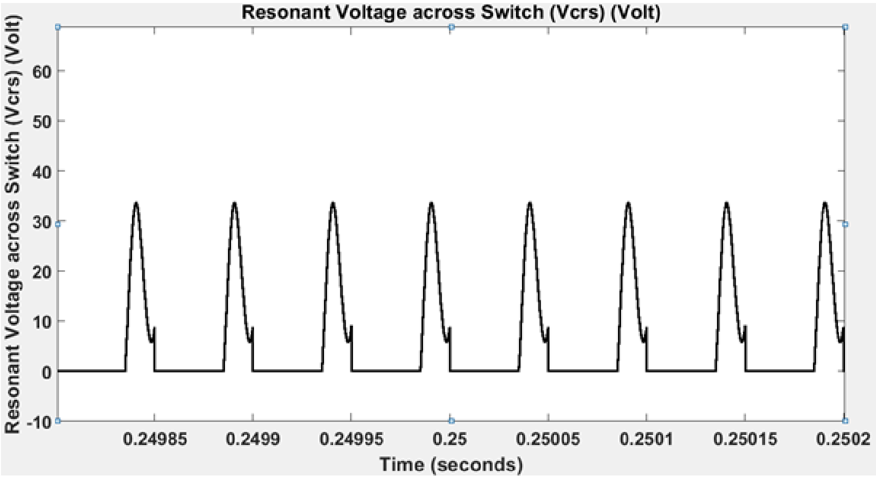

Fig. 3(e) - Resonant Voltage across diode (V_{crd}) of Buck ZVS MRC

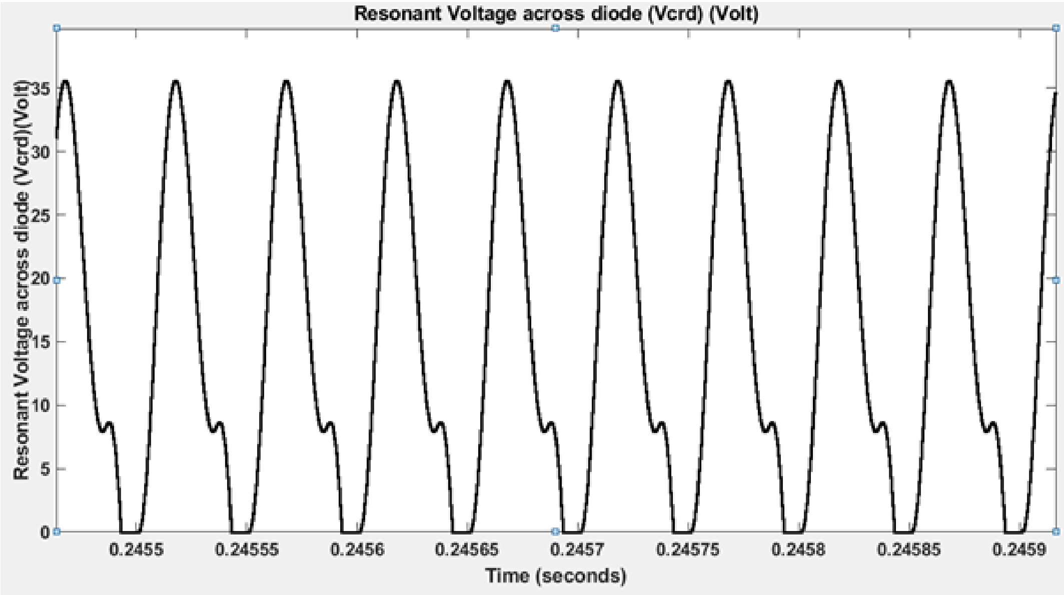

From Fig. 3(a), the average value of the inductor present is 0.15 A. The peak-peak value of the resonant inductor current present in Fig. 3(b) is 0.5 A and the frequency is 20 kHz. The average output voltage of Fig. 3(c) is 14 V. The peak resonant voltage across switch of Fig. 3(d) is 35 V with a frequency of 20 kHz. The peak resonant voltage across diode of Fig. 3(e) is 35 V with a frequency of 20 kHz. All these values logically obey equations.

The circuit diagram as seen in Fig. 1 is simulated directly in PSIM software without using the developed model. The simulated results of filter inductor current (I_L), Resonant Inductor current (I_{Lr}), Filter capacitor voltage (V_c), Resonant capacitor voltage across switch (V_{crs}) and Resonant capacitor voltage across diode (V_{crd}) are shown in Fig. 4(a) to 4(e).

Fig. 4(a) =- Filter Inductor Current (I_L) of Buck ZVS MRC

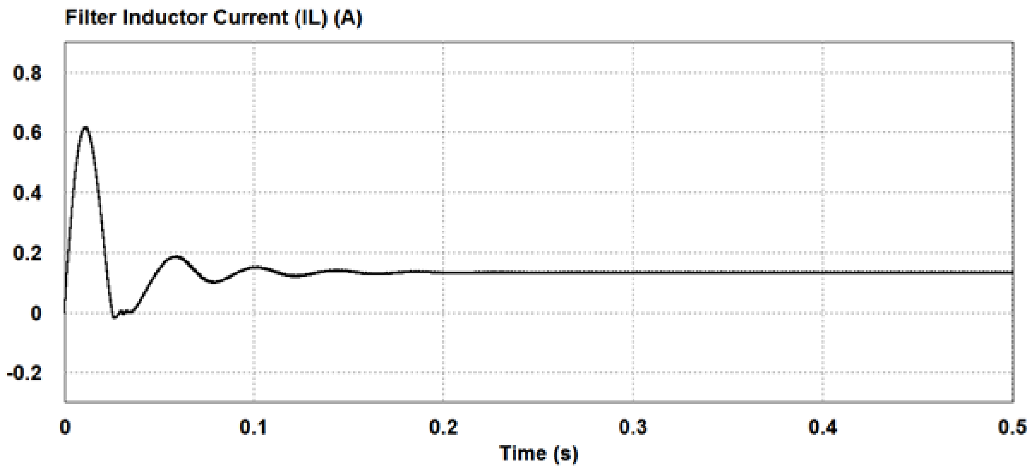

Fig. 4(b) - Resonant Inductor Current (I_{Lr}) of Buck ZVS MRC

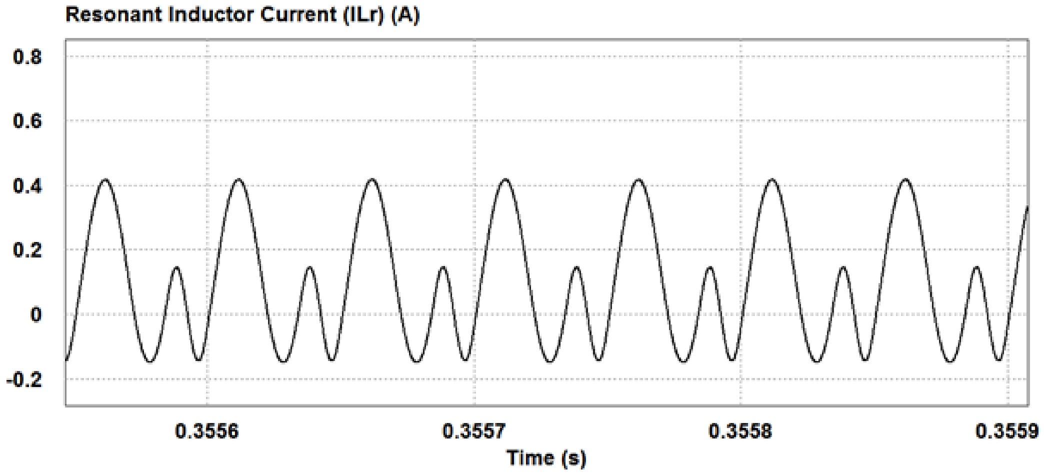

Fig. 4(c) - Filter Capacitor voltage (V_c) of Buck ZVS MRC

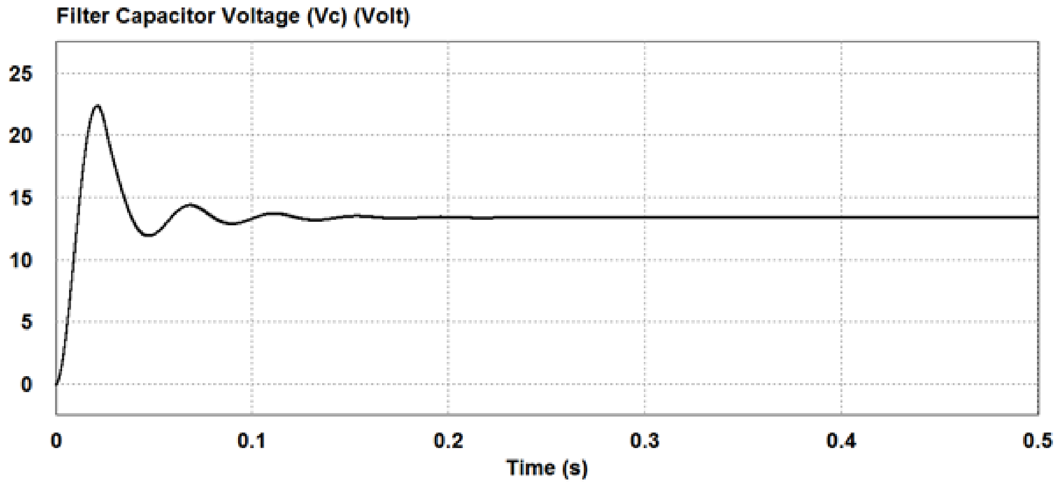

Fig. 4(d) - Resonant Voltage across switch (V_{crs}) of Buck ZVS MRC

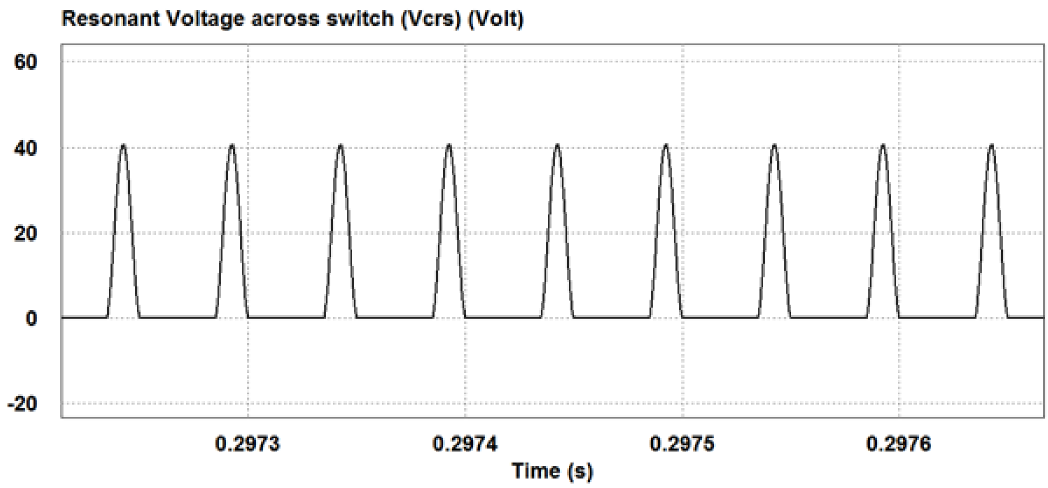

ISSN: 2237-0722
Vol. 11 No. 4 (2021)
Received: 19.05.2021 – Accepted: 11.06.2021

Fig. 4(e) - Resonant Voltage across diode (V_{crd}) of Buck ZVS MRC

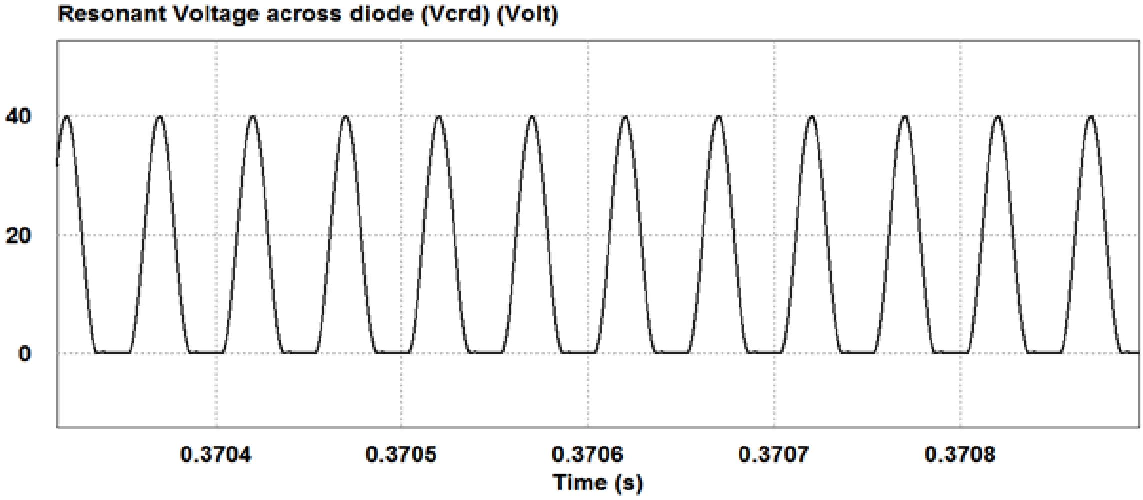

Fig. 4(a) reveal that the average inductor current value is 0.16 A. The maximum-maximum value of the resonant inductor current from Fig. 4(b) is 0.52 A and the frequency is 20 kHz. The average output voltage of Fig. 4(c) is 13 V. From Fig. 4(d), the peak resonant capacitor voltage across switch is 40 V, and the frequency is 20 kHz. From Fig. 4(e), the peak resonant capacitor voltage across diode is 40 V, and the frequency is 20 kHz. Both these values technically obey the equations.

6. Experimental Results and Analysis

Fig. 5(a) - Gate pulse Creation Circuit Using IC555

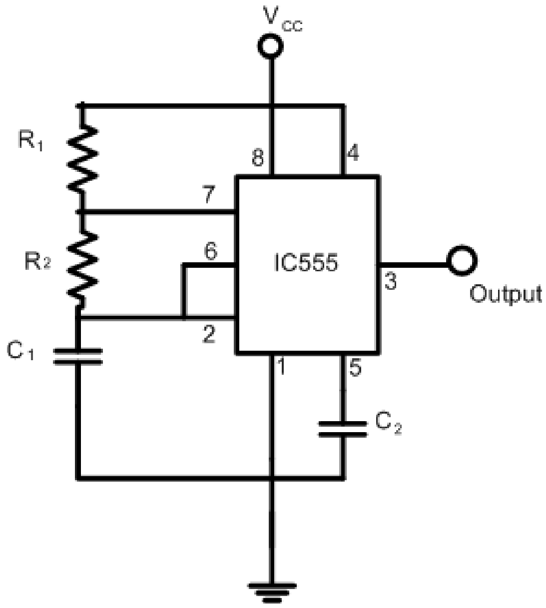

ISSN: 2237-0722
Vol. 11 No. 4 (2021)
Received: 19.05.2021 – Accepted: 11.06.2021

The hardware components are selected according to the specification parameters in Table 5. Switch (MOSFET) gate pulses are created from IC555 timer. As seen in Fig. 5(a), the IC is in Astable mode. ON time (t_1 in sec), OFF time (t_2 in sec), switching frequency (f_s) and duty cycle (d) are defined by (13) – (16) respectively. Given, $C_2 = C_1 = 0.01$ μF. Resistors R_1 and R_2 are potentiometers and are calibrated to produce the appropriate frequency and duty ratio pulses. The generated pulse is produced in Fig. 5(b). Fig. 6 displays the converter's experimental configuration along with the pulse generation circuit.

$$t_1 = \frac{(R_1 + R_2)}{1.443} C_1 \tag{13}$$

$$t_2 = \frac{R_2}{1.443} C_1 \tag{14}$$

$$f_s = 1/(t_2 + t_1) \tag{15}$$

$$d = \left(\frac{1 + R_2 / R_1}{1 + 2R_2 / R_1}\right) \tag{16}$$

Fig. 5(b) - Pulse of 70% duty cycle from circuit using IC555

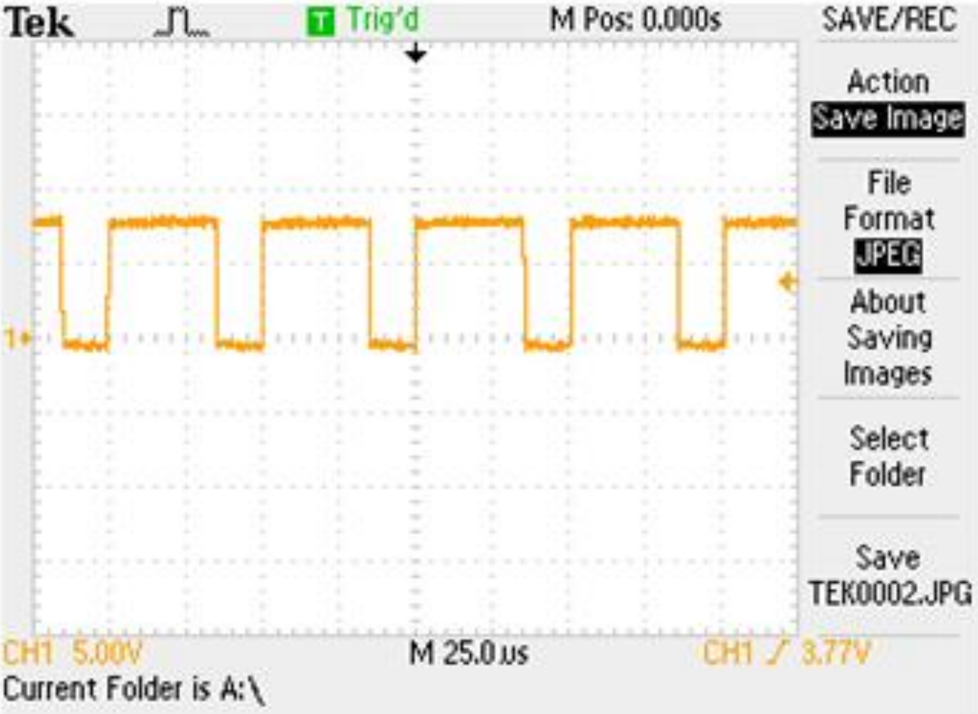

ISSN: 2237-0722
Vol. 11 No. 4 (2021)
Received: 19.05.2021 – Accepted: 11.06.2021

Fig. 6 - Experimental set up of Buck ZVS MRC

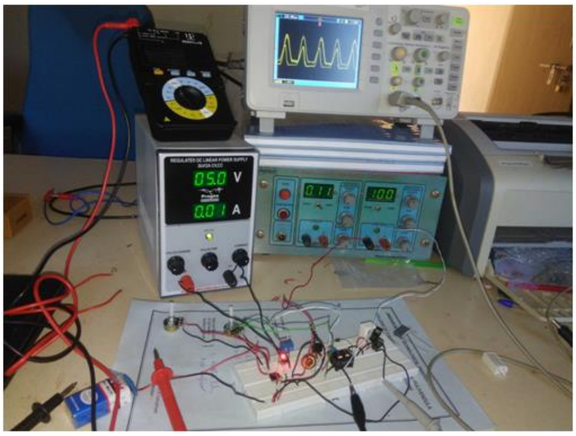

Fig. 7(a) - 7(e) display the plots of the filter inductor current (IL), resonant inductor conductor current (ILr), filter capacitor voltage (Vc), resonant switch capacitor voltage (Vcrs) and resonant diode capacitor voltage (Vcrd).

Fig. 7(a) - Filter Inductor Current (I_L) of Buck ZVS MRC

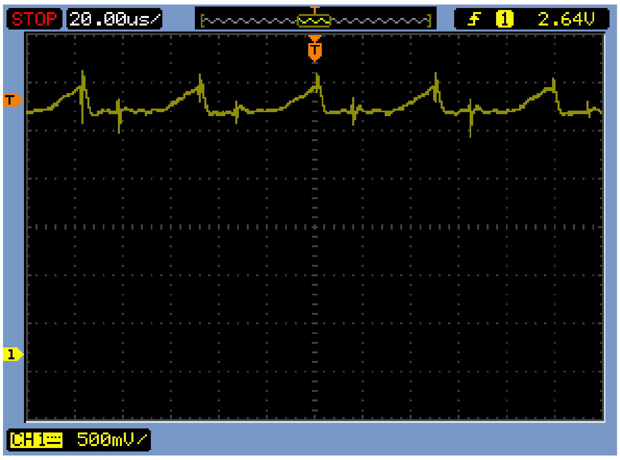

Fig. 7(b) - Resonant Inductor Current (I_{Lr}) of Buck ZVS MRC

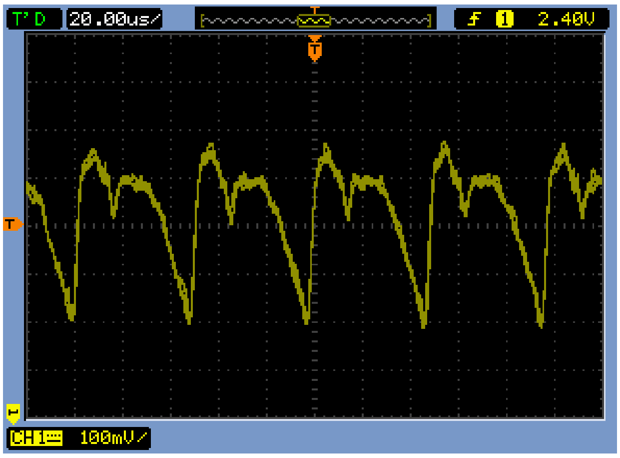

ISSN: 2237-0722
Vol. 11 No. 4 (2021)
Received: 19.05.2021 – Accepted: 11.06.2021

Fig. 7(c) - Filter Capacitor voltage (V_c) of Buck ZVS MRC

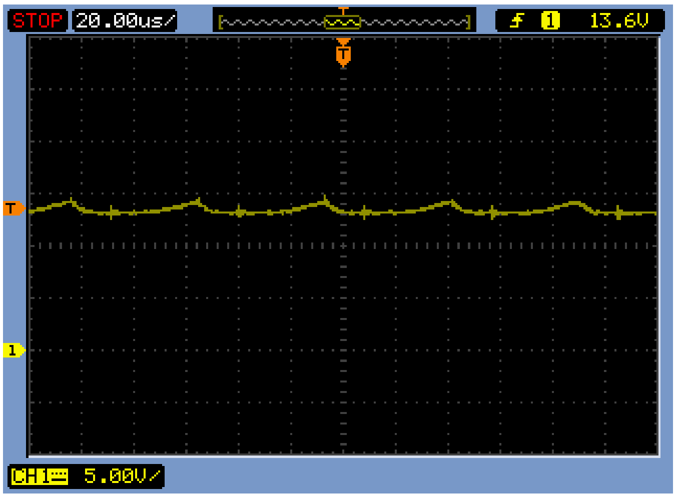

Fig. 7(d) - Resonant Voltage Across Switch (V_{crs}) of Buck ZVS MRC

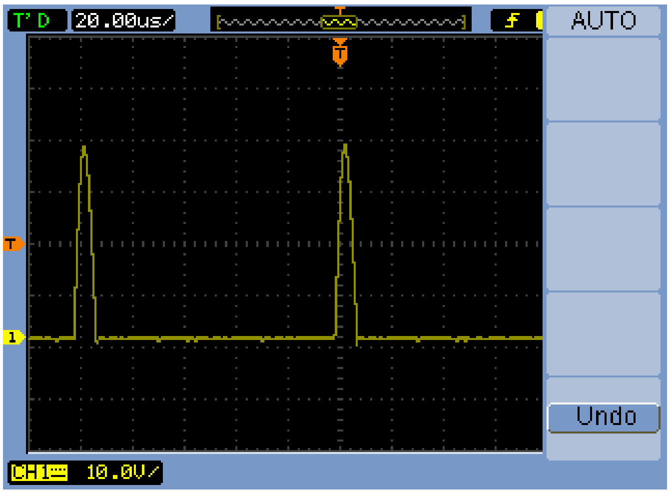

Fig. 7(e) - Resonant Voltage across diode (V_{crd}) of Buck ZVS MRC

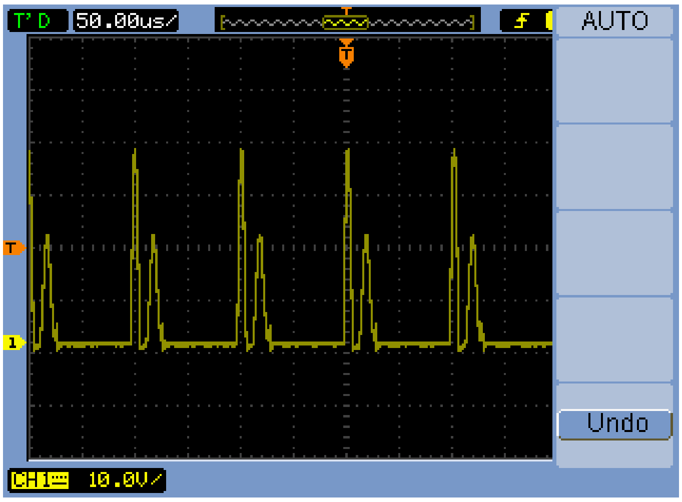

ISSN: 2237-0722
Vol. 11 No. 4 (2021)
Received: 19.05.2021 – Accepted: 11.06.2021

The inductor current (I_L) is calculated by using a current probe that is set at 100 mV/A. The average current to be calculated is 0.14 A. The Resonant Inductor current (I_{Lr}) was measured according to the same procedure and was 0.5 A (peak-peak).

7. Numerical Analysis of Results

The bond graph model results that were obtained in (MATLAB/SIMULINK), PSIM results and the results of the experimental buck ZVS MRC converter are presented in Table 6. The simulation results of the established MATLAB/SIMULINK bond graph model, simulated circuit model results in PSIM and experimental findings demonstrate the precision of the model developed in roughly the same way.

Table 6 - Buck ZVS MRC Converter

	MATLAB/SIMULINK	PSIM	Experimental
$I_{L(avg)}$	0.15 A	0.16 A	0.14 A
$I_{Lr\ (peak\text{-}peak)}$	0.5 A	0.52 A	0.5 A
$V_{c(avg)}$	14 V	13 V	19 V
$V_{crs\ (peak)}$	35 V	40 V	39 V
$V_{crd\ (peak)}$	35 V	40 V	39 V

8. Conclusion

A PWM converter suffers from high switching loss and heavy switching stress. The above problems can be solved by Quasi-resonant DC-DC converters by switching when the voltage and current are zero. Since there are some drawbacks of quasi-resonant converters including parasitic oscillations and capacitive turn on losses, Multi resonant DC-DC converters can be used to overcome. Buck ZVS MRC converter is modeled through bond graphs. An accurate large signal bond model of the Buck ZVS MRC converter has been constructed based on the bond graph drawing. This is how the State equations are developed using this graph. The bond graph model developed is simulated in MATLAB/SIMULINK for state variables filter inductor current (I_L), resonant inductor current (I_{Lr}), filter capacitor voltage (V_c), resonant capacitor voltages (V_{crs} and V_{crd}). The variable values and the profiles of state variables are verified by running the circuit model in PSIM and then comparing their simulation results with the experimental results to see if they match. The developed bond graph model results in MATLAB/SIMULINK are in direct agreement to prove its accuracy when used in a number of multi-domain applications of the converter, such as automotive and solar applications.

References

Mohan N, Undeland TM, Robbins W (2007). *Power Electronics: Converters Applications and Design*. Wiley & sons.

Severns R (2014). *Modern DC-to-DC Switched mode Power Converter Circuits*. Van Nostarnd Reinhold Electrical and Computer Science Engineering Series.

Kazimirczuk M (2015). *Pulse-Width Modulated DC-to-DC Power Converters*. Wiley and sons.

Liu KH, Lee FCY (1990). Zerovoltage switching technique in DC-to-DC converters. *IEEE Transactions on Power Electronics 5*(3), 293-304.

Todd PC, Lutz RW (1986). Practical resonant power converters: Theory and applications. In *Power technique Magazine*. 29-35.

Hua G, Lee FC (1995). Soft switching techniques in PWM converters. *IEEE Transactions on Industrial Electronics* 42(6), 595-603.

Tabisz WA, Lee FC (1989). Zero voltage switching multiresonant technique – A novel approach to improve performance of high frequency quasi-resonant converters. *IEEE Transaction on power electronics* 4(4), 450-458.

Mohan N, Robbins W, Undeland TM, Nilsen R, Mo O (1994). Simulation of power electronics and motion control systems: an overview. *Proceedings of the IEEE* 82(8), 1287-1302.

Maksiimovic D, Stankoviic AM, Thotuvelil VJ, Vergese GC (2001). Modelling and simulation of power electronic converters. *Proceedings of the IEEE* 89(6), 898-912.

Jin H (1997). Behavior Mode Simulation of Power Electronic Circuits. *IEEE Transections on Power Electornics* 12(3), 443-452.

Deskur JM (1997). PSpice Simulation of Power Electronic and Motion Control Systems. *ISIE97 Procedings of the IEEE International Symposium on Industrial Electornics*. Giumaraes, Portugal

Karnop DC, Margoliis DL, Rosenbirg RC (1990). *System Dynamics: A Unified Approach*. John Wiley and Sons.

Mukherjei A, Karmakar R (2000). *Modelling and Simulation of Engineering Systems through Bond Graphs.* Alpha Science International Limited.

Boretzzky W, Tanguyy GD, Thomaa JU (1995). Advances in bondgraph modelling theory, software, applications. *Journal of Mathematics and Computer in Simulation*, 39(5), 465-475.

Dellgedo M, Sira-Remiraz H (1998). A bond graph approach to the modelling and simulation of switch regulated dc-to-dc power supplies. *Simulation Practice and Theory*, 6(7), 631-646.

Allerd B, Hilalee H, Lin CC, Morelll H (1995). Power Converter average model computation using the bond graph and PetriNit Techniques. *Proceedings of PESC95 – Power Electronics Specialist Conference*, 830-836.

Umarikar AC, Umanand L (2005). Modelling of switching systems in bond graphs using the concept of switced power junctions. *Journal of the Frankliine Institute*. 342(2)., 131-147.

Umarikar AC, Umanand L (2005). Modelling of switched mode power converters using bond graphs. *IEE Proceedings - Electric Power Applications*. 152(1), 51-60.

Kazimeirczuk MK, Czarkawski D (2011). *Resonant Power Converters*. John Wiley & Sons

Umarikar AC, Mishra T, Umanand L (2006). Bondgraph Simulation and Symbolic Extraction tool box in MATLAB/SIMULINK. *Journal. Indian Institute of Science (IISc)*, 86(1), 45-68.